

# Shell model study of $T = 0$ states for $^{96}\text{Cd}$ by the nucleon-pair approximation

G. J. Fu,<sup>1,2,\*</sup> Y. Y. Cheng,<sup>2</sup> Y. M. Zhao,<sup>2,3,†</sup> and A. Arima<sup>2,4</sup>

<sup>1</sup>*School of Physics Science and Engineering, Tongji University, Shanghai 200092, China*

<sup>2</sup>*Shanghai Key Laboratory of Particle Physics and Cosmology, INPAC, Department of Physics and Astronomy, Shanghai Jiao Tong University, Shanghai 200240, China*

<sup>3</sup>*IFSA Collaborative Innovation Center, Shanghai Jiao Tong University, Shanghai 200240, China*

<sup>4</sup>*Musashi Gakuen, 1-26-1 Toyotama-kami Nerima-ku, Tokyo 176-8534, Japan*

(Received 9 March 2016; revised manuscript received 6 May 2016; published 25 August 2016)

In this paper we study the nucleon-pair approximation for  $T = 0$  states of  $^{96}\text{Cd}$  in the  $1p_{1/2}1p_{3/2}0f_{5/2}0g_{9/2}$  shell with the JUN45 interaction. The lowest seniority scheme and the isoscalar spin-one pair approximation are not enough to describe the states. The isoscalar spin-aligned pair approximation is reasonably good for the yrast  $2^+$ ,  $4^+$ ,  $6^+$ ,  $12^+$ ,  $14^+$ , and  $16^+$  states as pointed out previously. Not only the yrast positive-parity states but also nonyrast states and negative-parity states are well described by both the isovector pair approximation and the isoscalar pair approximation. We calculate overlaps between nucleon-pair basis states and shell-model wave functions. The largest overlaps and the corresponding nucleon-pair basis states are presented. We find that isovector spin-zero pairs, isovector spin-two pairs, and isoscalar spin-aligned pairs are the dominant building blocks in these states.

DOI: [10.1103/PhysRevC.94.024336](https://doi.org/10.1103/PhysRevC.94.024336)

## I. INTRODUCTION

The pairing correlation is very important in nuclear physics. Isovector nucleon pairs with spin  $J = 0$  are found to be dominant ingredients in low-lying states of semimagic nuclei [1], which has been emphasized by the seniority scheme [2], the generalized seniority scheme [1,3,4], the BCS theory [5–8], the interacting boson model [9], the broken pair model [10–12], and the nucleon-pair approximation of the shell model [13]. The isovector pairs with spin  $J = 0$  also play a key role in nuclear infinite matter. These facts are the consequences of the strong isovector  $J = 0$  pairing interaction between nucleons. See Refs. [14,15] for a comprehensive review.

In addition to the isovector  $J = 0$  pairing interaction, isoscalar  $J = 1$  and  $J = 2j$  (for a large- $j$  orbit) pairing interactions are strong. Therefore isoscalar deuteron-like  $J = 1$  pair approximation and isoscalar spin-aligned  $J = 2j$  pair approximation may provide us with proper scenario for low-lying states of  $N = Z$  nuclei. However, there has been no conclusive evidence for strong isoscalar  $J = 1$  pairing correlation. See Refs. [16–18] for a comprehensive review on proton-neutron pairing correlations.

In 2011 the level scheme of  $^{92}\text{Pd}$  was reported by Cederwall *et al.*, and the isoscalar spin-aligned nucleon pairs of the  $g_{9/2}$  orbit were suggested to be dominant building blocks in these states [19]. In Refs. [20–30] the importance of the isoscalar spin-aligned pairs was stressed for low-lying states of a few  $N = Z$  nuclei below  $^{100}\text{Sn}$ , such as  $^{92}\text{Pd}$  and  $^{96}\text{Cd}$ . On the other hand, the isoscalar spin-aligned pair approximation is not the unique picture for these low-lying states. References [20,31] showed that both the seniority scheme and the isoscalar

spin-aligned pair approximation are relevant in the ground state of  $^{92}\text{Pd}$  and  $^{96}\text{Cd}$  in the single- $j$  shell calculation. References [25,32] showed that both isovector pair approximation and isoscalar pair approximation provide good descriptions for the  $0_1^+$  and  $2_1^+$  states of  $^{92}\text{Pd}$  and  $^{96}\text{Cd}$ , and the ground rotational band of  $^{20}\text{Ne}$  and  $^{24}\text{Mg}$ . Such dual description is a consequence of the nonorthogonality feature of nucleon-pair basis. In Ref. [33] we studied nucleon-pair approximation for the ground state of  $^{20}\text{Ne}$ ,  $^{24}\text{Mg}$ ,  $^{32}\text{S}$ ,  $^{36}\text{Ar}$ ,  $^{44}\text{Ti}$ ,  $^{48}\text{Cr}$ ,  $^{60}\text{Zn}$ ,  $^{64}\text{Ge}$ ,  $^{92}\text{Pd}$ , and  $^{96}\text{Cd}$ . We found that the isovector  $J = 0$  pair approximation is relevant; the isoscalar spin-aligned pair approximation is relevant for the ground state of  $^{44}\text{Ti}$  and  $^{96}\text{Cd}$  but not good for that of  $^{48}\text{Cr}$  and  $^{92}\text{Pd}$ ; the isoscalar deuteron-like  $J = 1$  pair approximation is not good for the ground state of the even-even  $N = Z$  nuclei.

The purpose of this paper is to systematically study isovector and isoscalar pair approximations for  $T = 0$  states of  $^{96}\text{Cd}$ , in terms of the nucleon-pair approximation of the shell model with isospin symmetry [34]. We study not only the yrast positive-parity states but also nonyrast states and negative-parity states. We calculate level energies, wave functions, electromagnetic transition rates in nucleon-pair bases. This paper is organized as follows. In Sec. II we show the framework of the nucleon-pair approximation of the shell model. In Sec. III we study  $T = 0$  states of  $^{96}\text{Cd}$  in the  $1p_{1/2}1p_{3/2}0f_{5/2}0g_{9/2}$  shell with the JUN45 effective interaction [35]. In Sec. IV we summarize our results.

## II. FRAMEWORK

In this work  $^{96}\text{Cd}$  is regarded as a system of two valence-proton holes and two valence-neutron holes in the  $1p_{1/2}1p_{3/2}0f_{5/2}0g_{9/2}$  shell below the doubly closed-shell nucleus,  $^{100}\text{Sn}$ . In the nucleon-pair approximation with isospin symmetry [34],  $T = 0$  states of  $^{96}\text{Cd}$  are constructed by two

\* gifu@tongji.edu.cn

† Corresponding author: ymzhao@sjtu.edu.cn

pairs with given spins, isospins, and parities, i.e.,

$$|\Psi^{(I)}\rangle \equiv (A^{(J_1, T_1, \pi_1)^\dagger} \times A^{(J_2, T_2, \pi_2)^\dagger})^{(I)}|0\rangle, \quad (1)$$

where

$$A^{(J, T, \pi)^\dagger} = \sum_{ij} y(ij; JT\pi) A^{(J, T, \pi)^\dagger}(ij),$$

$$A^{(J, T, \pi)^\dagger}(ij) = (a_i^\dagger \times a_j^\dagger)^{(J, T, \pi)}. \quad (2)$$

Here  $|\Psi^{(I)^\dagger}\rangle$  denotes a state with spin  $I$ , isospin zero, and parity  $\pi_1 + \pi_2$ ;  $A^{(J, T, \pi)^\dagger}$  denotes a collective (or correlated) pair with spin  $J$ , isospin  $T$ , and parity  $\pi$ , and  $A^{(J, T, \pi)^\dagger}(ij)$  denotes a noncollective pair;  $a_i^\dagger$  denotes a valence hole on orbit  $i$ ;  $y(ij; JT\pi)$  is a set of structure coefficients.

The structure coefficients,  $y(ij; JT\pi)$ , of the collective pairs are determined as follows. For the isoscalar collective pairs,  $A^{(J, 0, \pi)^\dagger}$ , and the positive-parity isovector spin-zero pair,  $A^{(0, 1, +)^\dagger}$ , the structure coefficients are determined by minimizing the expectation value of the Hamiltonian,

$$\frac{\langle (A^{(J, T, \pi)^\dagger})^2 | H | (A^{(J, T, \pi)^\dagger})^2 \rangle}{\langle (A^{(J, T, \pi)^\dagger})^2 | (A^{(J, T, \pi)^\dagger})^2 \rangle}.$$

In order to obtain  $y(ij; JT\pi)$  for the isovector collective pairs except for the  $A^{(0, 1, +)^\dagger}$  pair, we diagonalize the Hamiltonian matrix in the  $(A^{(J, 1, \pi)^\dagger}(ij) \times A^{(0, 1, +)^\dagger})^{(J, 0, \pi)}|0\rangle$  space ( $A^{(J, 1, \pi)^\dagger}(ij)$  is the isovector noncollective pair with spin  $J$  and parity  $\pi$ ), with  $i, j$  running over all the single-particle orbits. The yrast-state wave function can be written by

$$\sum_{i \leq j} c(ij) (A^{(J, 1, \pi)^\dagger}(ij) \times A^{(0, 1, +)^\dagger})^{(J, 0, \pi)}|0\rangle,$$

and we assume  $y(ij; JT\pi) = c(ij)$ .

We study  $T = 0$  states of  $^{96}\text{Cd}$  in terms of the lowest seniority scheme, the spin-aligned pair approximation, the  $J_{\max}$  pair approximation, the spin-one pair approximation, the isovector pair approximation, the isoscalar pair approximation, and the shell model. In most cases we consider only positive-parity pairs, and the notation,  $A^{(J, T, \pi)^\dagger}$ , is reduced to  $A^{(J, T)^\dagger}$ .

(1) In the lowest seniority scheme, the wave function of states with spin  $I$ , isospin zero, and parity positive is written by

$$|\Psi_{\text{LS}}^{(I)}\rangle = (A^{(0, 1)^\dagger} \times A^{(I, 1)^\dagger})^{(I)}|0\rangle, \quad \text{for } I = 0, 2, 4, 6, 8, \quad (3)$$

where we use the subscript ‘‘LS’’ to represent ‘‘lowest seniority’’.  $A^{(0, 1)^\dagger}$  denotes a positive-parity isovector collective pair with  $J = 0$ , and  $A^{(I, 1)^\dagger}$  denotes a positive-parity isovector pair with  $J = I$ . It is noted that Eq. (3) is similar to the basis states used in the broken pair approximation [10–12].

(2) In the spin-aligned pair approximation, the wave function is written as

$$|\Psi_{\text{SA}}^{(I)}\rangle = (A^{(9, 0)^\dagger} \times A^{(9, 0)^\dagger})^{(I)}|0\rangle, \quad \text{for } I = 0, 2, 4, \dots, 16,$$

where we use the subscript ‘‘SA’’ to represent ‘‘spin aligned’’.  $A^{(9, 0)^\dagger}$  denotes the positive-parity isoscalar spin-aligned pair (namely the isoscalar pair with  $J = 9$ ) of the  $g_{9/2}$  orbit. The spin-aligned pair approximation has been studied for the yrast

$T = 0$  states of  $^{96}\text{Cd}$  in the  $1p_{1/2}1p_{3/2}0f_{5/2}0g_{9/2}$  shell in Ref. [25]. In this paper we show the results for comparison.

(3) In the  $J_{\max}$  pair approximation, we consider four positive-parity isoscalar  $J_{\max}$  pairs of single- $j$  orbits: the spin-1 pair of the  $1p_{1/2}$  orbit, the spin-3 pair of the  $1p_{3/2}$  orbit, the spin-5 pair of the  $0f_{5/2}$  orbit, and the spin-9 pair of the  $0g_{9/2}$  orbit. The pair basis state is written as

$$(A^{(J_1, 0)^\dagger} \times A^{(J_2, 0)^\dagger})^{(I)}|0\rangle.$$

By taking all possible combinations of the  $J_{\max}$  pairs, one gets a set of states. We diagonalize the Hamiltonian matrix in the space spanned by the states. The calculated wave functions in this space are denoted by  $|\Psi_{J_{\max}}^{(I)}\rangle$ .

(4) In the spin-one pair approximation, the pair basis states with spin  $I$ , isospin zero, and parity positive are constructed by at least one isoscalar spin-one pair, which are written as

$$(A^{(1, 0)^\dagger} \times A^{(I+1, 0)^\dagger})^{(I)}|0\rangle, \quad \text{for } I = 0, 2, 4, 6, 8,$$

$$(A^{(1, 0)^\dagger} \times A^{(I-1, 0)^\dagger})^{(I)}|0\rangle, \quad \text{for } I = 2, 4, 6, 8, 10,$$

$$(A^{(1, 0)^\dagger} \times A^{(I, 0)^\dagger})^{(I)}|0\rangle, \quad \text{for } I = 3, 5, 7, 9,$$

where  $A^{(1, 0)^\dagger}$ ,  $A^{(I \pm 1, 0)^\dagger}$ , and  $A^{(I, 0)^\dagger}$  denote positive-parity isoscalar pairs with  $J = 1$ ,  $I \pm 1$ , and  $I$ , respectively. We note that there is no  $I = 1$  state in the spin-one pair approximation. For  $I = 0, 3, 5, 7, 9, 10$  there is only one state, and for  $I = 2, 4, 6, 8$  there are two basis states. For the latter case we diagonalize the Hamiltonian matrix in the space spanned by the two basis states. The calculated wave functions in the spin-one pair approximation are denoted by  $|\Psi_{\text{SO}}^{(I)}\rangle$ , where we use the subscript ‘‘SO’’ to represent ‘‘spin one’’.

(5) In the isovector pair approximation, the pair basis state is constructed by isovector pairs, i.e.,

$$(A^{(J_1, 1, +)^\dagger} \times A^{(J_2, 1, \pi_2)^\dagger})^{(I)}|0\rangle,$$

where  $\pi_2$  is + for positive-parity states, and is – for negative-parity states.  $A^{(J_1, 1, +)^\dagger}$  and  $A^{(J_2, 1, +)^\dagger}$  denote positive-parity isovector pairs with spin  $J_1, J_2 = 0, 2, 4, 6, 8$ ;  $A^{(J_2, 1, -)^\dagger}$  denotes a negative-parity isovector pair with spin  $J_2 = 2, 3, 4, 5, 6, 7$ . By taking all possible combinations of the above isovector pairs, one gets a set of states, which are generally linearly dependent. We select a maximal linearly independent subset, which can be chosen in a few equivalent ways, and diagonalize the Hamiltonian matrix in the space spanned by the subset of states. The calculated wave functions in this space are denoted by  $|\Psi_{\text{IV}}^{(I)}\rangle$ , where we use the subscript ‘‘IV’’ to represent ‘‘isovector’’.

(6) In the isoscalar pair approximation, the pair basis state is constructed by isoscalar pairs, i.e.,

$$(A^{(J_1, 0, +)^\dagger} \times A^{(J_2, 0, \pi_2)^\dagger})^{(I)}|0\rangle,$$

where  $\pi_2$  is + for positive-parity states, and is – for negative-parity states.  $A^{(J_1, 0, +)^\dagger}$  and  $A^{(J_2, 0, +)^\dagger}$  denote positive-parity isoscalar pairs with  $J_1, J_2 = 1, 3, 5, 7, 9$ ;  $A^{(J_2, 0, -)^\dagger}$  denotes a negative-parity isoscalar pair with spin  $J_2 = 2, 3, 4, 5, 6, 7$ . The basis states are chosen in the same way as they are in the isovector pair approximation. We diagonalize the Hamiltonian

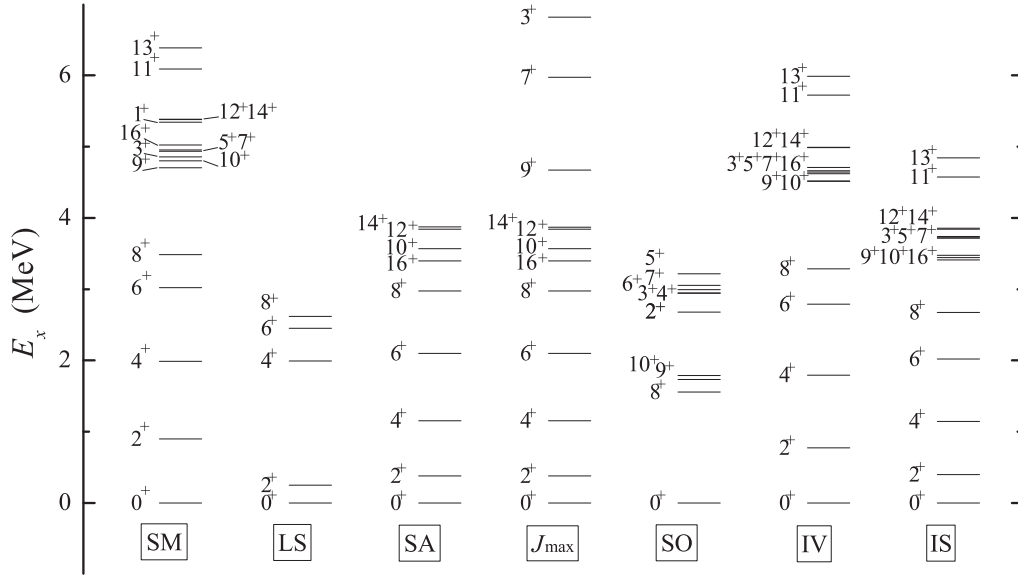


FIG. 1. Yrast  $T = 0$  positive-parity states of  $^{96}\text{Cd}$  calculated in the  $1p_{1/2}1p_{3/2}0f_{5/2}0g_{9/2}$  shell with JUN45 interaction. “SM” corresponds to the shell model, and “LS”, “SA”, “ $J_{\max}$ ”, “SO”, “IV”, and “IS” correspond to the lowest seniority scheme, the spin-aligned pair approximation, the  $J_{\max}$  pair approximation, the spin-one pair approximation, the isovector pair approximation, and the isoscalar pair approximation, respectively.

matrix in the isoscalar pair-truncated space, and the calculated wave functions are denoted by  $|\Psi_{\text{IS}}^{(I)}\rangle$ , where we use the subscript “IS” to represent “isoscalar”.

(7) We diagonalize the Hamiltonian matrix in the full  $1p_{1/2}1p_{3/2}0f_{5/2}0g_{9/2}$  shell-model space, and denote the calculated wave functions by  $|\Psi_{\text{SM}}^{(I)}\rangle$ , where we use the subscript “SM” to represent “shell model”.

### III. CALCULATIONS AND RESULTS

In this paper we call the quantity  $\langle\Psi_a|\Psi_b\rangle^2$  overlap between two wave functions,  $|\Psi_a\rangle$  and  $|\Psi_b\rangle$ . We calculate overlaps between the shell-model wave function  $|\Psi_{\text{SM}}\rangle$  and the pair-approximation wave functions  $|\Psi_{\text{LS}}\rangle$ ,  $|\Psi_{\text{SA}}\rangle$ ,  $|\Psi_{J_{\max}}\rangle$ ,  $|\Psi_{\text{SO}}\rangle$ ,  $|\Psi_{\text{IV}}\rangle$ ,  $|\Psi_{\text{IS}}\rangle$ . We also calculate the reduced electric-quadrupole transition probability, the electric-quadrupole moment, and the magnetic-dipole moment in the SM, LS, SA,  $J_{\max}$ , SO, IV, and IS spaces. We use the JUN45 effective interaction [35]; the effective charges are taken to be 1.5 for valence protons and 1.1 for valence neutrons, and the effective  $g$  factors are taken to be  $g_s = 5.586 \times q_s$ ,  $g_l = 1$  for valence protons and  $g_s = -3.826 \times q_s$ ,  $g_l = 0$  for valence neutrons, where  $q_s = 0.7$  is the quenching factor. For the yrast  $T = 0$  positive-parity states we present energy spectra in Fig. 1, the overlaps in Fig. 2, and the electromagnetic properties in Fig. 3; for the yrast  $T = 0$  negative-parity states we present the results in Figs. 4, 5, and 6, respectively.

#### A. Validity of the nucleon-pair approximation

Let us begin with the yrast  $T = 0$  positive-parity states of  $^{96}\text{Cd}$ . According to the shell-model result presented in Fig. 1, one sees nearly equal distances between the  $0_1^+$ ,  $2_1^+$ ,  $4_1^+$ ,  $6_1^+$  levels and a relatively smaller distance between the  $6_1^+$  and  $8_1^+$  levels. In Figs. 1 and 2 one sees the lowest seniority

scheme does not reproduce the spectra very well, and the overlaps between the shell-model wave functions and the lowest-seniority wave functions range between 0.45 and 0.80. The spin-one pair approximation is not enough to describe those  $T = 0$  states.

The spin-aligned pair approximation reproduce the equal distances between the  $2_1^+$ ,  $4_1^+$ ,  $6_1^+$  levels. The distance between the calculated  $6_1^+$  and  $8_1^+$  levels is too large, and the overlap  $\langle\Psi_{\text{SM}}|\Psi_{\text{SA}}\rangle^2$  for the  $8_1^+$  state is very small; the  $8_1^+$  state cannot be described by the spin-aligned pairs. The single- $0g_{9/2}$  shell calculation result showed that the spin-aligned pair

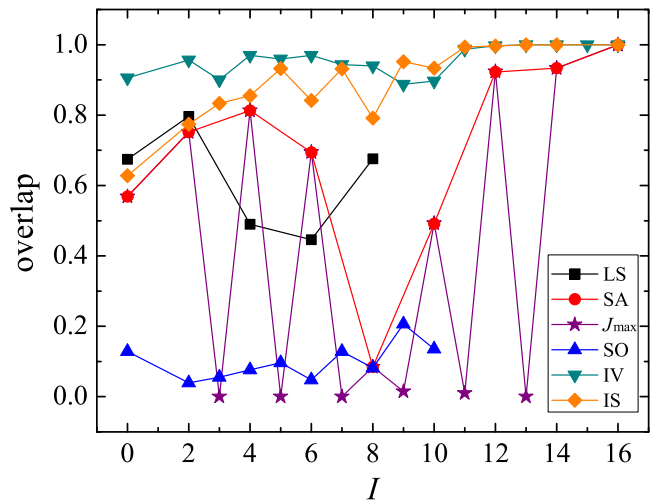


FIG. 2. Overlaps between wave functions obtained in the  $1p_{1/2}1p_{3/2}0f_{5/2}0g_{9/2}$  shell-model space and those obtained in nucleon-pair approximation subspaces, for the yrast  $T = 0$  positive-parity states of  $^{96}\text{Cd}$ . “LS”, “SA”, “ $J_{\max}$ ”, “SO”, “IV”, and “IS” are the same as in Fig. 1.

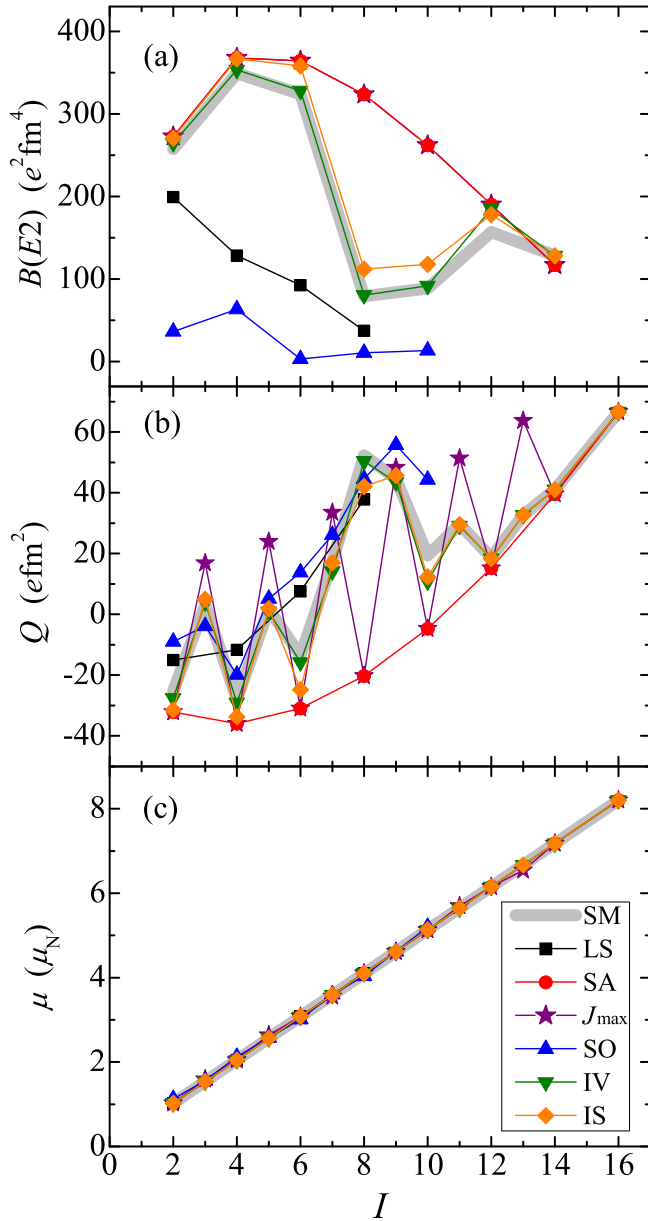


FIG. 3. Electromagnetic properties for the yrast  $T = 0$  positive-parity states of  $^{96}\text{Cd}$  calculated in the  $1p_{1/2}1p_{3/2}0f_{5/2}0g_{9/2}$  shell with JUN45 interaction: (a) reduced electric-quadrupole transition rates  $B(E2; I \rightarrow I - 2)$ , (b) electric-quadrupole moments  $Q$ , and (c) magnetic-dipole moments  $\mu$ . “SM”, “LS”, “SA”, “ $J_{\max}$ ”, “SO”, “IV”, and “IS” are the same as in Fig. 1.

approximation is responsible for the second  $T = 0$ ,  $8^+$  state [36]. In our  $1p_{1/2}1p_{3/2}0f_{5/2}0g_{9/2}$  shell calculation, the overlap  $\langle \Psi_{\text{SM}} | \Psi_{\text{SA}} \rangle^2$  for the second  $T = 0$ ,  $8^+$  state is equal to 0.73. For the  $12_1^+$ ,  $14_1^+$ , and  $16_1^+$  states, the overlaps  $\langle \Psi_{\text{SM}} | \Psi_{\text{SA}} \rangle^2$  are very close to 1, but the excitation energies obtained by the spin-aligned pair approximation are  $\sim 1.5$  MeV smaller than those obtained by the shell model. The reason is simple: the spin-aligned pair approximation shows an underbinding of  $\sim 1.5$  MeV for the ground state.

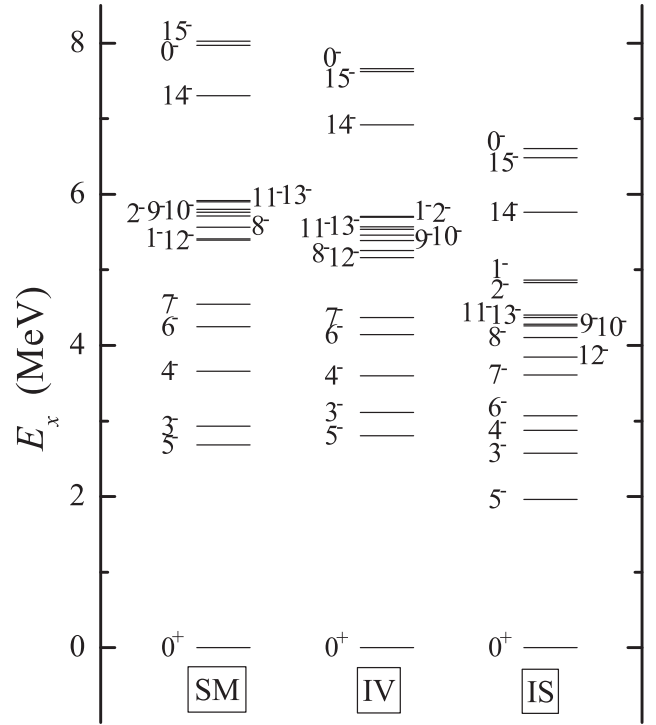


FIG. 4. Same as Fig. 1 except for the yrast  $T = 0$  negative-parity states.

For the  $0_1^+$ ,  $2_1^+$ ,  $4_1^+$ ,  $\dots$ ,  $16_1^+$  states, the level energies and the wave functions obtained by the  $J_{\max}$  pair approximation are very similar to those obtained by the spin-aligned pair approximation. For the  $3_1^+$ ,  $5_1^+$ ,  $\dots$ ,  $13_1^+$  states, the  $J_{\max}$  pair approximation is not good. This means the  $J_{\max}$  pairs of the  $1p_{1/2}$ ,  $1p_{3/2}$ , and  $0f_{5/2}$  orbits are not important in the yrast  $T = 0$  positive-parity states of  $^{96}\text{Cd}$ .

In the isovector pair approximation and the isoscalar pair approximation, we have considered more nucleon pairs. Thus

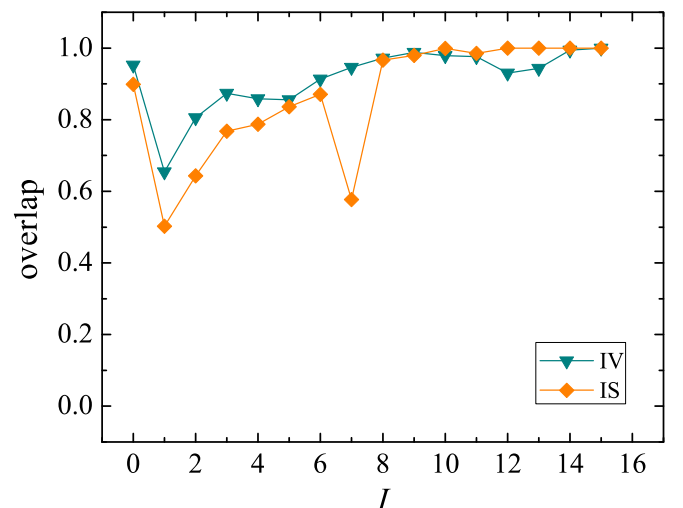


FIG. 5. Same as Fig. 2 except for the yrast  $T = 0$  negative-parity states.

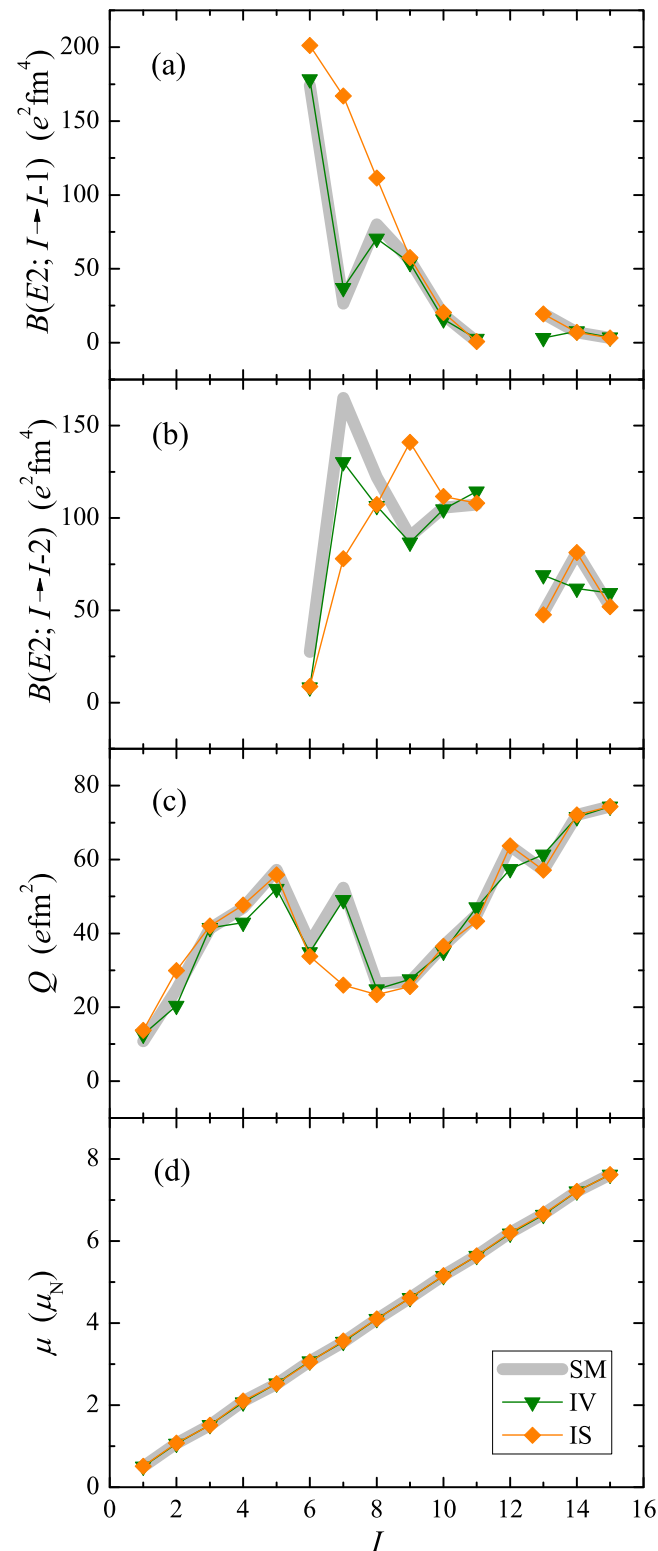


FIG. 6. Electromagnetic properties for the yrast  $T = 0$  negative-parity states of  $^{96}\text{Cd}$ : (a) reduced electric-quadrupole transition rates  $B(E2; I \rightarrow I - 1)$ , (b) reduced electric-quadrupole transition rates  $B(E2; I \rightarrow I - 2)$ , (c) electric-quadrupole moments  $Q$ , and (d) magnetic-dipole moments  $\mu$ . “SM”, “IV”, and “IS” are the same as in Fig. 1.

we expected these two pair approximations would provide good descriptions for low-lying states of  $^{96}\text{Cd}$ . This is indeed the case. The isoscalar pair approximation reasonably reproduces the spectra of the yrast  $T = 0$  positive-parity states, and the overlaps  $\langle \Psi_{\text{SM}} | \Psi_{\text{IS}} \rangle^2$  for most of the states are larger than 0.8. The isoscalar pair approximation results show an underbinding of  $\sim 1.5$  MeV for the ground state. The isovector pair approximation results are better, especially for the  $0_1^+$  and  $2_1^+$  states; the overlaps  $\langle \Psi_{\text{SM}} | \Psi_{\text{IV}} \rangle^2$  for the yrast  $T = 0$  positive-parity states are larger than 0.89.

In Fig. 3 one sees that the  $B(E2)$  values obtained by the lowest seniority scheme and those obtained by the spin-one pair approximation are much smaller than those obtained by the shell model. For  $I = 0, 2, 4, 12, 14, 16$ , the  $B(E2)$  and  $Q$  values obtained by the spin-aligned pair approximation are close to those by the shell model. But for  $I = 6$  and  $8$  they are very different, e.g., the  $Q$  value of the yrast  $8^+$  state obtained by the shell model is equal to  $52 e\text{fm}^2$ , and that by the spin-aligned pair approximation is equal to  $-20 e\text{fm}^2$ . For the second  $T = 0, 8^+$  state, the  $Q$  value obtained by the shell model is equal to  $-0.9 e\text{fm}^2$ . The  $B(E2)$  and  $Q$  values obtained by the isoscalar pair approximation are close to those by the shell model, except for the small deviations with  $I = 6, 8, 10$ . The  $B(E2)$  and  $Q$  values obtained by the isovector pair approximation are in very good accordance with those by the shell model. For the second  $T = 0, 8^+$  state, the  $Q$  value obtained by the isovector pair approximation is equal to  $-1.2 e\text{fm}^2$ , which is very close to the shell-model result.

Now we come to nonyrast  $T = 0$  positive-parity states. We calculate overlaps between the shell-model wave function  $|\Psi_{\text{SM}}\rangle$  and the pair-approximation wave functions  $|\Psi_{\text{IV}}\rangle$  and  $|\Psi_{\text{IS}}\rangle$ , for the second, third, and fourth  $T = 0, I^+$  states of  $^{96}\text{Cd}$ . The overlaps,  $\langle \Psi_{\text{SM}} | \Psi_{\text{IV}} \rangle^2$  or  $\langle \Psi_{\text{SM}} | \Psi_{\text{IS}} \rangle^2$ , larger than 0.5 are presented in Table I. One sees that the second  $T = 0$  states with  $I^+ = 4^+ - 8^+, 10^+, 12^+, 14^+$ , the third  $T = 0$  states with  $I^+ = 2^+, 6^+, 11^+, 12^+$ , and the fourth  $T = 0$  states with  $I^+ = 7^+ - 9^+$  are well described by both the isovector pair approximation and the isoscalar pair approximation. This dual description phenomenon is due to the nonorthogonality feature of nucleon-pair basis. The excitation energies obtained by the isoscalar pair approximation are much smaller than those calculated by the isovector pair approximation or the shell model, simply because the isoscalar pair approximation shows an underbinding of  $\sim 1.5$  MeV for the ground state.

We study the yrast  $T = 0$  negative-parity states of  $^{96}\text{Cd}$ . In Figs. 4, 5, and 6 one sees that both the isovector pair approximation and the isoscalar pair approximation provide good descriptions for most of the states. The excitation energies obtained by the isoscalar pair approximation are systematically smaller since the approximation underestimates the ground state energy in comparison to that of the shell model. In Fig. 5 one sees that  $\langle \Psi_{\text{SM}} | \Psi_{\text{IV}} \rangle^2$  is systematically larger than  $\langle \Psi_{\text{SM}} | \Psi_{\text{IS}} \rangle^2$  for the  $0^- - 7^-$  states.  $\langle \Psi_{\text{SM}} | \Psi_{\text{IV}} \rangle^2$  is not large for the  $1^-$  state;  $\langle \Psi_{\text{SM}} | \Psi_{\text{IS}} \rangle^2$  is not large for the  $1^-$ ,  $7^-$  state. We find large deviations between the  $B(E2)$  and  $Q$  values obtained by the isoscalar pair approximation and those by the shell model for  $I = 7$  (see in Fig. 6). The  $B(E2)$  and  $Q$  values obtained by the isovector pair approximation are very close to those by the shell model.



TABLE I. Nonyrast  $T = 0$  positive-parity states of  $^{96}\text{Cd}$  calculated in the  $1p_{1/2}1p_{3/2}0f_{5/2}0g_{9/2}$  shell with JUN45 interaction. The first column is spin and parity; the second column is the excitation energy obtained in the SM space; the third column is the overlap  $\langle\Psi_{\text{SM}}|\Psi_{\text{IV}}\rangle^2$ ; the fourth column is the excitation energy obtained in the IV space; the fifth column is the overlap  $\langle\Psi_{\text{SM}}|\Psi_{\text{IS}}\rangle^2$ ; the sixth column is the excitation energy obtained in the IS space. “SM”, “IV”, and “IS” are the same as in Fig. 1, and the excitation energies are in the unit of MeV.

$I^\pi$	$E_x$ (SM)	$\langle\Psi_{\text{SM}} \Psi_{\text{IV}}\rangle^2$	$E_x$ (IV)	$\langle\Psi_{\text{SM}} \Psi_{\text{IS}}\rangle^2$	$E_x$ (IS)
the second $T = 0$ positive-parity states					
$0^+$	2.03			0.50	2.70
$4^+$	4.47	0.87	4.28	0.74	3.55
$5^+$	5.88	0.94	5.58	0.83	4.66
$6^+$	4.38	0.95	4.13	0.78	3.45
$7^+$	5.80	0.85	5.62	0.88	4.53
$8^+$	4.28	0.97	3.96	0.92	2.96
$10^+$	5.38	0.71	5.19	0.96	3.92
$12^+$	6.27	0.98	5.91	1.00	4.74
$14^+$	7.03	1.00	6.63	1.00	5.49
the third $T = 0$ positive-parity states					
$0^+$	4.88	0.51	4.70		
$2^+$	4.38	0.78	4.02	0.70	3.47
$3^+$	6.67			0.52	5.57
$6^+$	5.74	0.90	5.46	0.86	4.47
$8^+$	5.20			0.58	4.20
$11^+$	7.37	0.99	6.98	1.00	5.83
$12^+$	7.34	0.97	6.98	0.99	5.81
$13^+$	13.21			0.97	11.57
$14^+$	10.98			1.00	9.44
the fourth $T = 0$ positive-parity states					
$4^+$	5.90	0.72	5.52	0.61	4.73
$5^+$	7.15			0.65	5.87
$6^+$	6.34			0.56	5.03
$7^+$	6.62	0.92	6.29	0.95	5.13
$8^+$	5.64	0.84	5.36	0.78	4.32
$9^+$	6.50	0.93	6.10	0.98	5.00
$10^+$	6.07			0.86	4.75
$11^+$	8.64			0.84	7.39

In Figs. 3(c) and 6(d) one sees an elegant linear relation between the magnetic-dipole moment,  $\mu$ , and the spin,  $I$ , in both the shell model result and the pair approximation results. In Fig. 3(c) we fit the magnetic-dipole moment values obtained by the shell model to the linear function  $\mu/\mu_N = aI + \epsilon$ , and we have  $a = 0.5129 \pm 0.0002$  and  $\epsilon = -0.0003 \pm 0.0012$ . Thus we have  $g \equiv \frac{\mu}{\mu_N I} \approx 0.5129$ . It is noticed that experimental values of the  $g$  factor are approximately equal to 0.5 for low-lying states of even-even  $N = Z$  nuclei [37]. This interesting phenomenon was also studied in terms of the collective model [38], the strong LS coupling [39], the single- $j$  shell model [40], and the attractive surface- $\delta$  interaction [41].

## B. The “optimal” nucleon-pair basis

Now we study the “optimal” nucleon-pair basis for the yrast  $T = 0$  states with either positive or negative parity.

Our purpose here is to find the “optimal” one-dimensional, two-dimensional, and three-dimensional nucleon-pair truncated subspaces, respectively, in which the wave function obtained by diagonalizing the JUN45 Hamiltonian matrix has the largest overlap with the shell-model wave function for the yrast states. We consider in total 26 nucleon pairs, including 13 isovector pairs with  $J^\pi = 0^+, 2^+, 4^+, 6^+, 8^+, 1^+, 3^+, 2^-, 3^-, 4^-, 5^-, 6^-, 7^-$ , and 13 isoscalar pairs with  $J^\pi = 1^+, 3^+, 5^+, 7^+, 9^+, 2^+, 4^+, 2^-, 3^-, 4^-, 5^-, 6^-, 7^-$ . We note that isovector pairs with  $J^\pi = 5^+, 7^+, 9^+, 0^-, 1^-, 8^-, 9^-$  or isoscalar pairs with  $J^\pi = 0^+, 6^+, 8^+, 0^-, 1^-, 8^-, 9^-$  do not survive in the  $1p_{1/2}1p_{3/2}0f_{5/2}0g_{9/2}$  shell.

The “optimal” one-dimensional nucleon-pair truncated subspace (alternatively, the “optimal” nucleon-pair basis state) for the yrast  $T = 0$ ,  $I^\pi$  state of  $^{96}\text{Cd}$  is determined through the following procedure. By taking all possible combinations of the 26 nucleon pairs, we get a large set of nucleon-pair basis states (denoted by  $|\Phi_i\rangle$ ). We calculate overlaps between the nucleon-pair basis states,  $|\Phi_i\rangle$ , and the shell-model wave function,  $|\Psi_{\text{SM}}\rangle$ , for the yrast  $T = 0$  states. We search for the largest overlap, and the corresponding nucleon-pair basis state is called the (first) optimal basis state (denoted by  $|\Phi_1\rangle$ ).

The second “optimal” basis state and the “optimal” two-dimensional subspace are determined as follows. For each nucleon-pair basis state  $|\Phi_i\rangle$  ( $\langle\Phi_i|\Phi_1\rangle^2 \neq 1$ ), we diagonalize the Hamiltonian matrix in the space spanned by  $|\Phi_1\rangle$  and  $|\Phi_i\rangle$ , and obtain the eigenstate with the lower energy, which is denoted by  $|\Phi'_i\rangle$ ; we calculate the overlap between  $|\Phi'_i\rangle$  and the shell-model wave function,  $|\Psi_{\text{SM}}\rangle$ . We search for the largest overlap, and the corresponding basis state,  $|\Phi_i\rangle$ , is called the second optimal basis state (denoted by  $|\Phi_2\rangle$ ); the space spanned by  $|\Phi_1\rangle$  and  $|\Phi_2\rangle$  is called the optimal two-dimensional subspace. The third optimal nucleon-pair basis state  $|\Phi_3\rangle$  is determined through the similar procedure, and the optimal three-dimensional subspace is spanned by  $|\Phi_1\rangle$ ,  $|\Phi_2\rangle$ , and  $|\Phi_3\rangle$ . We present the overlaps and the optimal nucleon-pair basis states,  $|\Phi_1\rangle$ ,  $|\Phi_2\rangle$ , and  $|\Phi_3\rangle$ , in Table II.

For the yrast  $T = 0$  states with  $I < 10$ , the overlaps between the first optimal basis states and the shell-model wave functions range between 0.50 and 0.86. For the yrast positive-parity states, all the first optimal basis states are constructed by positive-parity pairs.

For the  $0^+$ ,  $1^+$ ,  $2^+$ ,  $8^+$ ,  $3^-$ ,  $4^-$ , and  $5^-$  states, the first optimal basis state is the lowest-seniority wave function, although the overlaps are not larger than 0.80. For the  $4^+$ ,  $6^+$ ,  $2^-$ ,  $6^-$ , and  $7^-$  states, the lowest-seniority wave function becomes the second or the third optimal state. These results mean the isovector monopole pairing plays an important role in these states. For the  $0^+$  state, the second and third optimal basis states are constructed by two  $A^{(2,1,+)\dagger}$  pairs and two  $A^{(1,0,+)\dagger}$  pairs, respectively. For the  $4^+-8^+$ ,  $10^+$ ,  $0^-$ ,  $2^-7^-$  states, the  $A^{(2,1,+)\dagger}$  pair is also a key building block in the second and/or third optimal basis states. These results indicate that the isovector quadrupole pairing is also important.

For the  $4^+-6^+$ ,  $10^+-13^+$ ,  $2^-$ ,  $6^-$ ,  $8^-12^-$ , and  $14^-$  states, the isoscalar spin-aligned pair is highly relevant. In these states the first optimal basis state contains at least one  $A^{(9,0,+)\dagger}$  pair. For the  $8^-14^-$  states, most of the first three optimal

TABLE II. The “optimal” nucleon-pair basis states for the yrast  $T = 0$  states of  $^{96}\text{Cd}$ . “ $(J, T, \pi)$  in  $|\Phi_i\rangle$ ” means the spins, isospins, and parities of the nucleon pairs in the  $i$ th optimal basis state,  $|\Phi_i\rangle$ .

$I^\pi$	$(J, T, \pi)$ in $ \Phi_1\rangle$	overlap	$(J, T, \pi)$ in $ \Phi_2\rangle$	overlap	$(J, T, \pi)$ in $ \Phi_3\rangle$	overlap
$0^+$	(0,1,+)(0,1,+)	0.67	(2,1,+)(2,1,+)	0.90	(1,0,+)(1,0,+)	0.95
$1^+$	(0,1,+)(1,1,+)	0.73	(3,1,-)(4,1,-)	0.78	(2,1,+)(1,1,+)	0.80
$2^+$	(0,1,+)(2,1,+)	0.80	(9,0,+)(9,0,+)	0.90	(6,0,-)(6,0,-)	0.92
$3^+$	(2,1,+)(4,1,+)	0.85	(6,1,+)(8,1,+)	0.90	(4,0,-)(6,0,-)	0.94
$4^+$	(9,0,+)(9,0,+)	0.81	(0,1,+)(4,1,+)	0.88	(2,1,+)(2,1,+)	0.94
$5^+$	(9,0,+)(7,0,+)	0.82	(2,1,+)(6,1,+)	0.91	(2,1,+)(4,1,+)	0.94
$6^+$	(9,0,+)(9,0,+)	0.69	(0,1,+)(6,1,+)	0.90	(2,1,+)(4,1,+)	0.96
$7^+$	(2,1,+)(6,1,+)	0.72	(2,1,+)(8,1,+)	0.94	(1,0,+)(7,0,+)	0.99
$8^+$	(0,1,+)(8,1,+)	0.68	(2,1,+)(8,1,+)	0.81	(2,1,+)(6,1,+)	0.89
$9^+$	(2,1,+)(8,1,+)	0.74	(9,0,+)(3,0,+)	0.89	(9,0,+)(1,0,+)	0.98
$10^+$	(9,0,+)(9,0,+)	0.49	(2,1,+)(8,1,+)	0.70	(5,0,+)(7,0,+)	0.83
$11^+$	(9,0,+)(3,0,+)	0.81	(4,1,+)(8,1,+)	1.00	(9,0,+)(7,0,+)	1.00
$12^+$	(9,0,+)(9,0,+)	0.92	(6,1,+)(8,1,+)	1.00	(6,0,-)(6,0,-)	1.00
$13^+$	(9,0,+)(5,0,+)	1.00	(9,0,+)(4,0,+)	1.00		
$14^+$	(6,1,+)(8,1,+)	0.97	(9,0,+)(5,0,+)	1.00		
$0^-$	(5,0,+)(5,0,-)	0.86	(2,1,+)(2,1,-)	0.93	(2,0,+)(2,0,-)	0.97
$1^-$	(2,1,+)(3,1,-)	0.50	(2,0,+)(3,0,-)	0.66	(3,0,+)(4,0,-)	0.76
$2^-$	(9,0,+)(7,0,-)	0.52	(2,1,+)(4,1,-)	0.70	(0,1,+)(2,1,-)	0.85
$3^-$	(0,1,+)(3,1,-)	0.60	(2,1,+)(3,1,-)	0.76	(1,0,+)(4,0,-)	0.86
$4^-$	(0,1,+)(4,1,-)	0.68	(2,1,+)(4,1,-)	0.84	(8,1,+)(4,1,-)	0.86
$5^-$	(0,1,+)(5,1,-)	0.59	(2,1,+)(5,1,-)	0.79	(1,0,+)(5,0,-)	0.83
$6^-$	(9,0,+)(4,0,-)	0.70	(2,1,+)(5,1,-)	0.77	(0,1,+)(6,1,-)	0.83
$7^-$	(2,1,+)(5,1,-)	0.33	(0,1,+)(7,1,-)	0.56	(2,1,+)(7,1,-)	0.77
$8^-$	(9,0,+)(4,0,-)	0.84	(9,0,+)(2,0,-)	0.90	(9,0,+)(6,0,-)	0.93
$9^-$	(9,0,+)(4,0,-)	0.83	(9,0,+)(5,0,-)	0.90	(9,0,+)(2,0,-)	0.94
$10^-$	(9,0,+)(4,0,-)	0.93	(9,0,+)(2,0,-)	0.98	(9,0,+)(6,0,-)	0.99
$11^-$	(9,0,+)(4,0,-)	0.80	(9,0,+)(5,0,-)	0.90	(8,1,+)(3,1,-)	0.96
$12^-$	(9,0,+)(4,0,-)	0.99	(9,0,+)(6,0,-)	0.99	(9,0,+)(3,0,-)	1.00
$13^-$	(8,1,+)(5,1,-)	0.92	(9,0,+)(4,0,-)	0.96	(8,1,+)(6,1,-)	0.99
$14^-$	(9,0,+)(6,0,-)	0.98	(9,0,+)(5,0,-)	1.00		

basis states contain at least one  $A^{(9,0,+)\dagger}$  pair. Interestingly we find that the first optimal basis state of the  $6^-$ , and  $8^-$ – $12^-$  states is constructed by one  $A^{(9,0,+)}$  pair and the other  $A^{(4,0,-)}$  pair.

Finally we find that the overlaps between the optimal basis states and the shell-model wave functions for the  $1^+$ ,  $8^+$ ,  $10^+$ ,  $1^-$ – $7^-$  states are relatively small.

#### IV. SUMMARY

In this paper we systematically study low-lying  $T = 0$  states (including both positive-parity states and negative-parity states) of  $^{96}\text{Cd}$  by using the nucleon-pair approximation of the nuclear shell model with isospin symmetry. We calculate these states in the  $1p_{1/2}1p_{3/2}0f_{5/2}0g_{9/2}$  shell with the JUN45 effective interaction. We present overlaps between wave functions obtained by the shell model and those by the nucleon-pair approximation. We compare level spectra and electromagnetic properties obtained by these two methods.

The lowest seniority scheme and the isoscalar spin-one pair approximation are not enough to describe those  $T = 0$  states. The isoscalar spin-aligned pair approximation is reasonably good for the yrast  $2^+$ ,  $4^+$ ,  $6^+$ ,  $12^+$ ,  $14^+$ ,  $16^+$  states, but not for

the yrast  $8^+$  and  $10^+$  states. In the single- $0g_{9/2}$  shell calculation [36] the spin-aligned pair approximation is responsible for the second  $T = 0$ ,  $8^+$  state; in our calculation the overlap between the spin-aligned pair approximation wave function and the shell-model wave function is 0.73 for this state. Both the isovector pair approximation and the isoscalar pair approximation provide a good description for the yrast  $T = 0$  positive-parity states, the yrast  $T = 0$  negative-parity states, and a few nonyrast  $T = 0$  positive-parity states. In particular, the level spectra, wave functions, and electromagnetic properties obtained by the isovector pair approximation are very close to those obtained by the shell model. We show a linear relation between the magnetic-dipole moment and the spin for states of  $^{96}\text{Cd}$ , i.e.,  $\mu/\mu_N = 0.5129I - 0.0003$ , this regularity is in accordance with that found in Refs. [37–41].

We study the “optimal” nucleon-pair basis for the yrast  $T = 0$  states of  $^{96}\text{Cd}$ . We present the overlaps between the optimal nucleon-pair basis states and the shell-model wave functions. According to our calculations, the overlap between the first optimal basis state and the shell-model wave function ranges between 0.50 and 0.86 for the states with  $I < 10$ . For the positive-parity states, all the first optimal basis states are constructed by positive-parity pairs. We find the  $A^{(0,1,+)\dagger}$ ,  $A^{(2,1,+)\dagger}$ , and  $A^{(9,0,+)\dagger}$  pairs are highly relevant in the optimal

nucleon-pair basis states, which indicates that the isovector monopole pairing, the isovector quadrupole pairing, and the isoscalar spin-aligned pairing coexist in low-lying states of  $^{96}\text{Cd}$ .

It is well known that the generalized seniority scheme [1,3,4] and the broken pair model [10–12] work very well for low-lying states of semimagic nuclei. For example, the overlap between the lowest-seniority wave function and the shell-model wave function ranges between 0.92 and 0.96 for  $0_1^+$  and  $2_1^+$  states [33,42]. The simple picture of nucleon-pair states and the so-called hierarchical structure in yrast states of semimagic nuclei were pointed out in Ref. [43]. In this work we show that for low-lying states (with  $I < 10$ ) of the  $N = Z$  even-even nucleus,  $^{96}\text{Cd}$ , there is no single nucleon-pair basis

state which is responsible for more than 86% of the shell-model wave functions.

## ACKNOWLEDGMENTS

This work was supported by the National Natural Science Foundation of China under Grants No. 11505113 and No. 11225524, the 973 Program of China under Grant No. 2013CB834401, Shanghai Key Laboratory of Particle Physics and Cosmology under Grants No. 15DZ2272100 and No. 11DZ2260700, the Program of Shanghai Academic Research Leader under Grant No. 16XD1401600, and China Postdoctoral Science Foundation under Grant No. 2015M580319.

- 
- [1] I. Talmi, *Simple Models of Complex Nuclei* (Harwood Academic, Chur, 1993).
- [2] G. Racah, *Phys. Rev.* **62**, 438 (1942); **63**, 367 (1943).
- [3] S. Shlomo and I. Talmi, *Nucl. Phys. A* **198**, 81 (1972).
- [4] I. Talmi, *Nucl. Phys. A* **172**, 1 (1971).
- [5] J. Bardeen, L. N. Cooper, and J. R. Schrieffer, *Phys. Rev.* **106**, 162 (1957); **108**, 1175 (1957).
- [6] A. Bohr, B. R. Mottelson, and D. Pines, *Phys. Rev.* **110**, 936 (1958).
- [7] S. T. Belyaev, *Mat. Fys. Medd. K. Dan. Vidensk. Selsk.* **31**, 11 (1959).
- [8] A. B. Migdal, *Nucl. Phys.* **13**, 655 (1959).
- [9] A. Arima and F. Iachello, *Adv. Nucl. Phys.* **13**, 139 (1984); F. Iachello and A. Arima, *The Interacting Boson Model* (Cambridge University Press, Cambridge, 1987).
- [10] Y. K. Gambhir, A. Rimini, and T. Weber, *Phys. Rev.* **188**, 1573 (1969).
- [11] Y. K. Gambhir, S. Haq, and J. K. Suri, *Ann. Phys. (NY)* **133**, 154 (1981).
- [12] K. Allart, E. Boeker, G. Bonsignori, M. Saroia, and Y. K. Gambhir, *Phys. Rep.* **169**, 209 (1988).
- [13] J. Q. Chen, *Nucl. Phys. A* **626**, 686 (1997); Y. M. Zhao, N. Yoshinaga, S. Yamaji, J. Q. Chen, and A. Arima, *Phys. Rev. C* **62**, 014304 (2000).
- [14] D. J. Dean and M. Hjorth-Jensen, *Rev. Mod. Phys.* **75**, 607 (2003).
- [15] Y. M. Zhao and A. Arima, *Phys. Rep.* **545**, 1 (2014).
- [16] D. D. Warner, M. A. Bentley, and P. Van Isacker, *Nat. Phys.* **2**, 311 (2006).
- [17] S. Frauendorf and A. O. Macchiavelli, *Prog. Part. Nucl. Phys.* **78**, 24 (2014).
- [18] C. Qi and R. Wyss, *Phys. Scr.* **91**, 013009 (2016).
- [19] B. Cederwall *et al.*, *Nature* **469**, 68 (2011).
- [20] K. Neergård, *Phys. Rev. C* **88**, 034329 (2013).
- [21] S. Zerguine and P. Van Isacker, *Phys. Rev. C* **83**, 064314 (2011).
- [22] C. Qi, J. Blomqvist, T. Bäck, B. Cederwall, A. Johnson, R. J. Liotta, and R. Wyss, *Phys. Rev. C* **84**, 021301(R) (2011).
- [23] C. Qi, *Prog. Theor. Suppl.* **196**, 414 (2012).
- [24] Z. X. Xu, C. Qi, J. Blomqvist, R. J. Liotta, and R. Wyss, *Nucl. Phys. A* **877**, 51 (2012).
- [25] G. J. Fu, J. J. Shen, Y. M. Zhao, and A. Arima, *Phys. Rev. C* **87**, 044312 (2013).
- [26] L. Coraggio, A. Covello, A. Gargano, and N. Itaco, *Phys. Rev. C* **85**, 034335 (2012).
- [27] B. S. Nara Singh *et al.*, *Phys. Rev. Lett.* **107**, 172502 (2011).
- [28] K. Ogawa, *Phys. Rev. C* **28**, 958 (1983).
- [29] P. Van Isacker, *Phys. Scr., T* **150**, 014042 (2012).
- [30] P. Van Isacker, *Int. J. Mod. Phys. E* **22**, 1330028 (2013).
- [31] K. Neergård, *Phys. Rev. C* **90**, 014318 (2014).
- [32] G. J. Fu, Y. M. Zhao, and A. Arima, *Phys. Rev. C* **90**, 054333 (2014).
- [33] G. J. Fu, Y. M. Zhao, and A. Arima, *Phys. Rev. C* **91**, 054322 (2015).
- [34] G. J. Fu, Y. Lei, Y. M. Zhao, S. Pittel, and A. Arima, *Phys. Rev. C* **87**, 044310 (2013).
- [35] M. Honma, T. Otsuka, T. Mizusaki, and M. Hjorth-Jensen, *Phys. Rev. C* **80**, 064323 (2009).
- [36] C. Qi, J. Blomqvist, T. Bäck, B. Cederwall, A. Johnson, R. J. Liotta, and R. Wyss, *Phys. Scr., T* **150**, 014031 (2012).
- [37] B. A. Brown, *J. Phys. G* **8**, 679 (1982).
- [38] A. Bohr and B. R. Mottelson, *Nuclear Structure* (Benjamin, New York, 1969), Vol. I; *Nuclear Structure* (Benjamin, New York, 1975), Vol. II.
- [39] A. Arima, *Hyperfine Interact.* **4**, 151 (1978).
- [40] S. Yeager, S. J. Q. Robinson, L. Zamick, and Y. Y. Sharon, *Europhys. Lett.* **88**, 52001 (2009).
- [41] L. Zamick, B. Kleszyk, Y. Y. Sharon, and S. J. Q. Robinson, *Phys. Rev. C* **90**, 027305 (2014).
- [42] Y. Lei, Z. Y. Xu, Y. M. Zhao, and A. Arima, *Phys. Rev. C* **82**, 034303 (2010).
- [43] Y. Y. Cheng, Y. M. Zhao, and A. Arima, *Phys. Rev. C* **94**, 024307 (2016); Y. Y. Cheng, C. Qi, Y. M. Zhao, and A. Arima, *ibid.* **94**, 024321 (2016).